

## Solidification Velocities in Deeply Undercooled Silver

Wai-Lun Chan,<sup>1,\*</sup> Robert S. Averback,<sup>1</sup> David G. Cahill,<sup>1</sup> and Yinon Ashkenazy<sup>2</sup>

<sup>1</sup>*Department of Materials Science and Engineering, University of Illinois at Urbana-Champaign, Urbana, Illinois 61801, USA*

<sup>2</sup>*Racah Institute of Physics, Hebrew University of Jerusalem, 91904 Jerusalem, Israel*

(Received 18 November 2008; revised manuscript received 17 January 2009; published 6 March 2009)

We measure the solidification velocity of pure Ag as a function of undercooling temperature from the melting point ( $T_m = 1235$  K) to  $0.6T_m$  using ultrafast, pump-probe laser experiments. The thickness of the liquid layer, while it solidifies, is measured using optical third harmonic generation. We show that velocity reaches a maximum value at  $0.85T_m$ , and then remains nearly constant with additional undercooling. These results contradict simple collision-limited models, but they are in good agreement with molecular dynamics simulations presented here, which show that the crystallization velocity depends weakly on temperature from  $0.85T_m$  to less than  $\approx 0.1T_m$ .

DOI: 10.1103/PhysRevLett.102.095701

PACS numbers: 64.70.D-, 61.20.Lc, 61.80.Ba, 81.30.Fb

Solidification of metals is one of the most fundamental processes in materials science, and indeed it has been extensively studied for many decades. For pure metals, most of these studies have been limited to the liquid-solid phase transition close to equilibrium [1–3], which is largely due to the difficulty in avoiding crystallization at deep undercoolings. Even after carefully removing heterogeneous nucleation sites, pure metals can only be quenched to about  $0.8T_m$  before they solidify [4] ( $T_m$  is the melting temperature). As a consequence, many questions about solidification at ultradeep undercoolings remain unanswered. For example: What is the maximum rate of solidification and what determines this limit? Does the behavior change after falling below the glass temperature and is it possible to quench a pure metal below its glass temperature? The answers to these questions can significantly impact our fundamental understanding of supercooled liquids and glasses, as well as the development of far-from-equilibrium materials. While studies of multicomponent metallic alloys can help to answer some of these questions [5], the solidification kinetics of alloys is generally far more complex owing to the effects of chemical ordering and differences in atomic size and mass. In this Letter, we report on the solidification velocity in Ag as a function of temperature, achieving supercoolings as deep as  $0.6T_m$ . We compare these results with models of solidification and to our molecular dynamics simulations, which are carried out from the melting temperature to  $\approx 50$  K.

In order to reach deep undercoolings, we employ an ultrafast (femtosecond) laser to melt a very thin layer of metal on the surface, 10–20 nm. The heat is then allowed to dissipate into the remainder of the sample. By heating just a very thin layer of material, very rapid quench rates can be achieved. The degree of undercooling during solidification, moreover, can be readily controlled by changing the thickness of the thin films, which are grown on a dielectric substrate. A few preliminary studies using picosecond (ps) lasers to measure the solidification velocity in noble [6] and transition [7] metals have been reported previously;

however, these studies have been largely qualitative, and the velocity was not measured as a function of undercooling temperature. Nanosecond (ns) lasers, on the other hand, have been used extensively to study the solidification in alloys [2] and semiconductors [8], but they heat hundreds of nm's of material and the degree of undercooling that could be achieved was small.

The samples used here are Ag thin films, epitaxially grown on MgO (001) substrates. They are melted by fs laser pulses, with a wavelength of 800 nm and a pulse width of 140 fs. A time-delayed probe beam is positioned at the center of the pump beam to measure the thickness of the liquid layer as a function of time, which we do using the optical third-order harmonic (TH) generation of light. Since the (001) orientated Ag generates TH light but the isotropic liquid phase does not [9], this technique is very sensitive to the liquid-solid phase transformation, and it provides an accurate measure on the solidification velocity. The thickness of the liquid layer,  $d$ , can be related to the normalized TH signal by a simple exponential relationship

$$I(t)/I_0 = \exp(-d/d_0), \quad (1)$$

where  $I(t)$  is the TH intensity, and  $I_0$  is the TH intensity without the pump pulse. The parameter  $d_0$  is the extinction depth of the signal, which has been calibrated experimentally by a series of Ag/Fe/Ag multilayer samples to be 6.9 nm. The details of the calibration experiments are reported in Ref. [10]. In this calibration, we have verified the exponential relationship in Eq. (1), and showed that the  $d_0$  measured at low probe fluence is consistent with the theoretical prediction obtained from the measured optical constants of Ag. A schematic of the experimental setup is shown in Fig. 1.

Plotted in Fig. 2 on a semilog scale is the TH signal as a function of time for three samples of thicknesses: 75, 157, and 800 nm. The slopes, as seen from Eq. (1), represent the resolidification velocities. The calculated value of  $d$  as a function of time is indicated on the right axis. The signal decreases rapidly in the first 30–50 ps, representing the

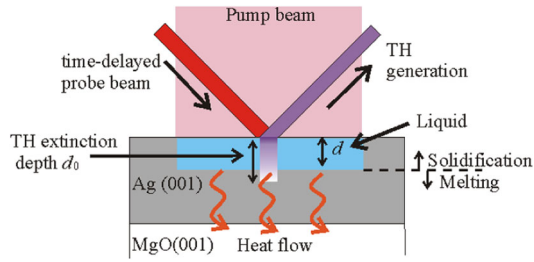


FIG. 1 (color online). A schematic of the experiment setup. The pump beam, which is  $\approx 10$  times larger in size than the probe beam, is used to melt the Ag. Optical TH generation is used to measure the thickness  $d$  of the liquid layer.

melting of the sample. The fluence used to melt the two thicker samples is  $0.46 \text{ J cm}^{-2}$ . A slightly smaller fluence,  $0.39 \text{ J cm}^{-2}$ , was used for the thinner sample. The smaller amount of energy required to melt the thinner sample is a consequence of the heat confinement by the Ag-MgO interface on a sub-100 ps time scale (the interface and substrate are poor heat conductors).

Considering the fast electron dynamics in Ag, the observed  $d$  ( $\approx 20 \text{ nm}$ ) at the end of melting is surprisingly small. The small  $d$  results from a transient high electron scattering rate [10] and a strong electron-phonon (e-ph) coupling [11] when the  $d$ -band electrons are initially excited by the laser. Details of the melting dynamics can be found in Ref. [10]. Here, we consider only the solidification process. For  $t > 50 \text{ ps}$ , the undercooled liquid starts to recrystallize and the TH signal recovers uniformly in this plot, indicating that the velocity of the interface is nearly constant during solidification. We will therefore refer only to the average velocity  $v_{av}$  in what follows. The process is completed by  $t \approx 200\text{--}300 \text{ ps}$ . The signal does not fully recover at  $t \approx 1 \text{ ns}$ , but it does so, however, before  $t \approx 1 \text{ s}$ . We attribute the degradation in signal at  $t = 1 \text{ ns}$  to the production of quenched-in defects (presumably vacancies) during solidification; such defects have been observed in the MD simulations discussed both below and elsewhere [12]. With the high vacancy mobility in Ag [13], these transient, nonequilibrium defects can anneal out at room temperature in less than 1 s. Finally, the loss of material by ablation was less than the sensitivity of postirradiation measurements using electron microscopy,  $\approx 1 \text{ nm}$  per pulse.

While the solidification velocities found in Fig. 2 appear nearly constant for an individual sample,  $v_{av}$  does depend on the thickness of the sample. The change in  $v_{av}$  is due to the different undercoolings attained in different samples. The conductance of heat through the thin Ag film is much faster than through the Ag-MgO interface and the MgO substrate. During the solidification, therefore, the heat spreads rapidly across the entire Ag film, but only a small amount of heat can transport across the Ag-MgO interface. Larger undercoolings are thus achieved in thicker film. By finding  $v_{av}$  as a function of film thickness, we can determine the solidification velocity as a function of temperature.

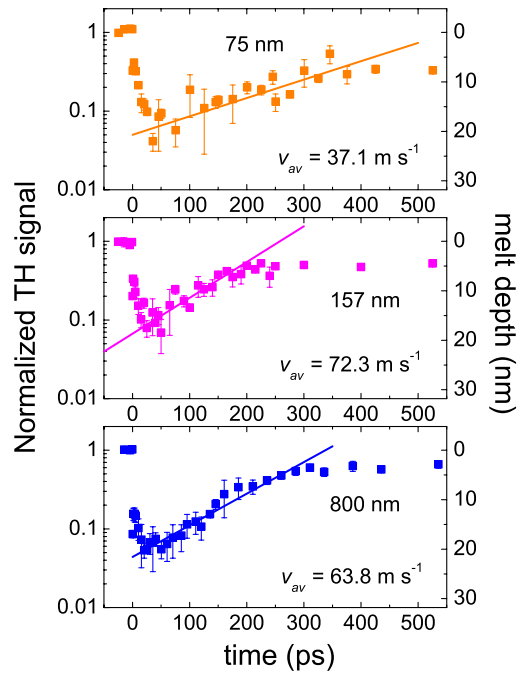


FIG. 2 (color online). The TH signal as a function of time measured for samples with three different thicknesses of the Ag layer. The converted melt depth is shown on the axis on the right. The average resolidification velocity is indicated by the solid lines.

The amount of undercooling is not directly measured, but it can be estimated rather well by solving the 1D heat diffusion equation. We calculate the lattice temperature using a two temperature model (TTM) [14]. As we have pointed out previously [10], Ag has a small e-ph coupling constant; therefore, during the rapid cooling of the shallow surface region, the electron temperature ( $T_e$ ) and phonon temperatures ( $T_p$ ) can fall out of equilibrium. In our TTM model, we observe that  $T_p$  can be a few hundred degrees higher than  $T_e$  near the liquid-solid interface. A similar, but opposite, effect is observed in the modeling of melting in superheated Ni [15]. At the beginning of the simulation, a liquid-solid interface is located at the maximum melt-depth observed in experiment. During the first 30 ps, the interface velocity is assumed to increase linearly [16], and after which it is allowed to move with a velocity equal to the average velocity  $v_{av}$  observed in experiments (Fig. 2). The latent heat of fusion is deposited uniformly into the phonons in a region  $\pm 5 \text{ nm}$  around the liquid-solid interface. This length is chosen based on the interface thickness and the phonon mean-free path [17]; it is also consistent with the width of the temperature spike around the interface observed in our MD simulations. Further details of the TTM can be found in Ref. [10]. Here, we highlight how we experimentally determine some of the input parameters that are not available in literature but which influence the calculated temperature profiles.

The calculated interface temperature depends, first of all, on the total energy initially deposited in the Ag film.

The amount of energy absorbed, however, is not readily available since the reflectivity of a fs pulse can change at very high laser fluences [18]. We determined the energy absorbed in the sample by measuring the temperature rise induced by laser irradiation of a very small, insulated sample using calorimetry. The details of this experiment will be reported elsewhere [19]. The absorption at the melting fluence is found to be 5.7% ( $\approx 3$  times larger than that in the low fluence limit). Note that this change is not a consequence of melting, which occurs only long after the laser pulse, but rather it is due to the extreme excitation of the electronic system.

Next, we need the initial temperature distribution. At  $t = 0$  ps, the liquid layer is assumed to be at the melting temperature  $T_m$ . The initial temperature across the Ag film is then determined using a power law relationship,  $T(t = 0) = T_m(x_0/x)^n$ , where  $x_0$  is the initial melt depth and  $x$  is the distance from the surface. The exponent  $n$  is fit using the constraint that the total energy in the film equals the absorbed fluence. Depending on film thicknesses,  $n$  ranges from 1.206 (800 nm Ag) to 0.002 (60 nm Ag), i.e., for our thinnest sample, the entire Ag film is heated nearly to  $T_m$ . This temperature distribution resembles the distribution calculated by our melting model after the initial melting [10]. Replacing the initial distribution with similar functions, but without changing the total energy absorbed, does not significantly alter the cooling rate. For example, using a Gaussian distribution results in a difference of only  $\approx 40$  K in the undercooling of the 800 nm film. A final parameter in the model is the interface conductance of the Ag/MgO interface, which is determined by time-resolved thermal reflectance measurement [20]. The conductance determined at room temperature is  $0.3 \text{ GW m}^{-2} \text{ K}^{-1}$ ; values at other temperatures are obtained by assuming it is proportional to the average temperature at the interface—as observed for Cu/sapphire interfaces [20].

Figure 3 shows the calculated phonon temperature at the liquid-solid interface as a function of time for samples with three different thicknesses. The thicker the sample, the lower is the liquid-solid interface temperature. An initial quenching rate of  $\approx 5 \times 10^{12} \text{ K s}^{-1}$  is found for the 800 nm-thick sample. The time at which the solidification front reaches the surface is labeled by arrows in the figure. The temperature rises just before this time since the latent heat is deposited in a thinner region as the liquid-solid interface moves toward the surface. A similar temperature rise has been observed in MD-TTM simulations [12]. The average crystallization temperature for each sample is taken to be the average temperature from  $t = 30$  ps to the time when the solidification ends. The first 30 ps is neglected because it mainly corresponds to the ramping up in the solidification velocity as it changes from melting to solidification (the minima in Fig. 2). This region is not included when we fit the average solidification velocity measured in the experiment.

With the average temperature obtained by the above model, and the average velocity obtained in Fig. 2, we

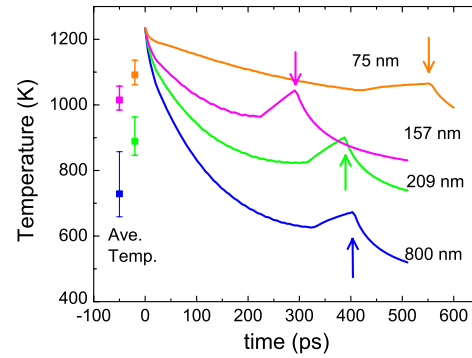


FIG. 3 (color online). The temperature at the liquid-solid interface as a function of time, calculated using the heat model described in the text. The arrows indicate the end of the solidification. The average temperatures over the whole period of solidification are indicated by the solid symbols on the left. The error bars above (below) the symbols represent the mean deviations from the average temperature during the period with temperatures above (below) the average temperature.

can plot the solidification velocity as a function of temperature. This is shown in Fig. 4 for temperatures as low as  $T \approx 750 \text{ K}$  (or  $\approx 0.6T_m$ ). The solidification velocity is also obtained as a function of temperature using MD simulation (see Ref. [21] for details); these data are shown in Fig. 4 as circles. The agreement between experiment and simulation is quite good; note that there are no adjustable parameters. The velocity increases approximately linearly from  $T_m$  to  $0.85T_m$ , and then it becomes insensitive to temperature with further decrease in temperature. The long plateau observed in Fig. 4 explains why the experimental solidification velocity remains nearly constant as a function of time even though Fig. 3 shows that the liquid-solid interface temperature can vary by  $\approx 200$ – $300 \text{ K}$  during solidification. This also justifies the use of an average undercooling temperature to plot the experimental data in Fig. 4.

Although continuum models for solidification have been developed for more than 50 years, none of these models have been experimentally verified in a pure metal at deep undercooling. It has long been assumed that the solidification rate in pure is controlled by collision-limited kinetics [6,22,23]. Furthermore, it is often accepted that there is no energy barrier for an atom to move across the liquid-solid interface. Under these assumptions, the velocity can be written as

$$v(T) = C \sqrt{\frac{3kT}{m}} [1 - \exp(-\Delta\mu/kT)], \quad (2)$$

where  $C$  is a geometric factor on the order of 1,  $m$  is the atomic mass, and  $\Delta\mu$  is the free energy different between the solid and liquid phase. This relation is shown as the solid line in Fig. 4. Because of the weak  $(T)^{1/2}$  dependence, the velocity continues to increase until  $T < 0.3T_m$ ; this clearly disagrees with the experimental and simulation data shown in Fig. 4.

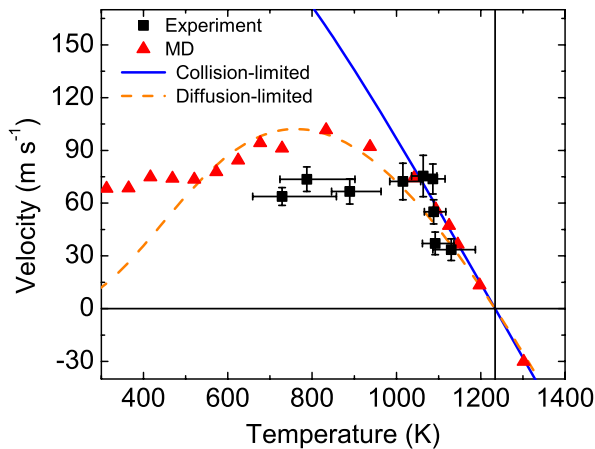


FIG. 4 (color online). Solidification velocity versus the temperature. The experimental data (squares) show reasonable agreement to the MD simulations (triangles). However, it clearly deviates from the collision-limited model (the blue solid line). If we assume the motion of the atom across the interface is thermally activated (with an activation barrier = 0.12 eV), the predicted velocity is shown as the dashed line.

If a barrier exists in the energy landscape for an atom to move from the liquid to the solid, one can replace the square root term in Eq. (2) by an exponential term  $A \exp(-E/kT)$  [24], where  $E$  represents the barrier height. In fact, such a barrier is proposed to exist in solidification of covalent materials such as Si [8]. By setting  $E = 0.12$  eV and  $A = 1300$   $\text{m s}^{-1}$ , indicated by the orange (dashed) line in Fig. 4, we see that above 600 K, the velocity agrees well with the MD simulation and the experimental data. The existence of an activation barrier, therefore, can explain why the solidification velocity reaches its maximum at a relatively high temperature. Such a barrier, however, indicates that the velocity should diminish at lower temperatures, which disagrees with the MD simulations. We note that, in Ag, the glass transition temperature  $T_g \approx 600$  K [25]. The discrepancy between the continuum models and the MD data perhaps suggests that the solidification mechanisms for the liquid and glass states may be very different.

In conclusion, we have measured the solidification velocity as a function of temperature down to  $0.6T_m$  using a fs laser. The results agree well with MD simulation. The solidification velocity for  $T < 0.8T_m$  clearly deviates from the collision-limited model that has been well accepted for pure metals. Our current results are consistent with models that include an activation barrier for an atom to cross the solid-liquid interface, although the MD simulations indicate that such a model, if valid for a supercooled liquid, must break down at the glass temperature.

This work was supported by the U.S. DOE-NNSA under Grant No. DE-FG52-06NA26153 and the U.S. DOE-BES under Grants No. DE-FG02-05ER46217. Sample characterization was carried out in part in the FS-MRL Central Facilities, University of Illinois, which are partially sup-

ported by the U.S. DOE under Grants No. DE-FG02-07ER46453 and No. DE-FG02-07ER46471.

\*wlchan@uiuc.edu

- [1] B. Chalmers, *Principles of Solidification* (John Wiley & Son, New York, 1964), p. 91–125.
- [2] P. M. Smith and M. J. Aziz, *Acta Metall. Mater.* **42**, 3515 (1994).
- [3] B. T. Bassler, W. H. Hofmeister, and R. J. Bayuzick, *Mater. Sci. Eng. A* **342**, 80 (2003).
- [4] D. Turnbull and R. E. Cech, *J. Appl. Phys.* **21**, 804 (1950); K. K. Leung, C. P. Chiu, and H. W. Kui, *Scr. Metall. Mater.* **32**, 1559 (1995).
- [5] H. Assadi and A. L. Greer, *Nature (London)* **383**, 150 (1996); H. Assadi, S. Reutzel, and D. M. Herlach, *Acta Mater.* **54**, 2793 (2006).
- [6] C. A. MacDonald, A. M. Malvezzi, and F. Spaepen, *J. Appl. Phys.* **65**, 129 (1989).
- [7] M. B. Agranat *et al.*, *Appl. Phys. A* **69**, 637 (1999).
- [8] J. Y. Tsao *et al.*, *Phys. Rev. Lett.* **56**, 2712 (1986).
- [9] P. N. Butcher and D. Cotter, *The Elements of Nonlinear Optics* (Cambridge University Press, Cambridge, 1990).
- [10] W.-L. Chan *et al.*, *Phys. Rev. B* **78**, 214107 (2008).
- [11] Z. Lin, L. V. Zhigilei, and V. Celli, *Phys. Rev. B* **77**, 075133 (2008).
- [12] Z. Lin, R. A. Johnson, and L. V. Zhigilei, *Phys. Rev. B* **77**, 214108 (2008).
- [13] P. Ehrhart, in *Atomic Defects in Metals*, edited by H. Ullmaier, Landolt-Bornstein New Series Vol. 25 (Springer-Verlag, Berlin, 1991), p. 203.
- [14] S. I. Anisimov, B. L. Kapeliovich, and T. L. Perel'man, *Sov. Phys. JETP* **39**, 375 (1974).
- [15] D. S. Ivanov and L. V. Zhigilei, *Phys. Rev. Lett.* **98**, 195701 (2007).
- [16] The resultant undercooling is insensitive to the function that we use to increase the velocity from 0 at  $t = 0$  ps to the average velocity at  $t = 30$  ps.
- [17] The phonon mean-free path is estimated to be  $\approx 3$  nm. The interface thickness observed in MD simulation  $\approx 2$  nm, which is defined as the thickness of the region containing both the liquid and solid atoms.
- [18] T. Ao *et al.*, *Phys. Rev. Lett.* **96**, 055001 (2006).
- [19] W.-L. Chan, R. S. Averback, and D. G. Cahill (to be published).
- [20] B. C. Gundrum, D. G. Cahill, and R. S. Averback, *Phys. Rev. B* **72**, 245426 (2005).
- [21] Y. Ashkenazy and R. S. Averback, *Europhys. Lett.* **79**, 26005 (2007).
- [22] S. R. Coriell and D. Turnbull, *Acta Metall.* **30**, 2135 (1982).
- [23] J. Q. Broughton, G. H. Gilmer, and K. A. Jackson, *Phys. Rev. Lett.* **49**, 1496 (1982).
- [24] J. Frenkel, *Kinetic Theory of Solids* (Oxford University Press, New York, 1946).
- [25] This was determined from the MD simulations by rapidly cooling a liquid system and monitoring the heat capacity as a function of temperature. At  $T_g$ , the heat capacity changes rapidly within a few tens of degree, which gives a clear indication of  $T_g$ .